Table 3 Summary of the clinical bone assessment.

Study	Group		Defect fill			Histological analysis			CT analysis	
			Base line (mm)	Change from base line (mm)	Percent vertical defect fill (%)	Woven bone (%)	Lamellar bone (%)	Bone substitute mineral (%)	Bone density at 4 months (mg/cm³)	Bone density 6 months post-functional loading (mg/cm³)
Simion et al.										
Control	—		—	—	—	—	—	—		
Test	rhPDGF-BB/Bio-Oss® + autogenous bone	Depth	20	ND	ND	ND	ND	ND		
		Width	15	ND	ND					
Byun et al.										
Control	—		—	—	—	—	—	—		
Test	rhPDGF-BB/β-TCP + autogenous bone	Depth	ND	ND	ND	ND	ND	ND		
		Width	ND	ND	ND					
Fagan et al.										
Control	—		—	—	—	—	—	—		
Test	rhPDGF-BB/FDBA	Depth	15	ND	ND	48	19	14		
		Width	8	ND	ND					
Boyne et al.										
Control	Autogenous bone graft	Height	11.29 ± 4.12	ND	ND				350 ± 243	448 + 213
		Width at 1/4	4.66 ± 2.75	ND	ND					
		Width at 1/2	10.17 ± 2.98	ND	ND					
		Width at 3/4	10.56 ± 3.17	ND	ND					
	rhBMP-2/ACS 0.75 mg/ml	Height	9.47 ± 5.72	ND	ND				84 ± 50	456 ± 131
		Width at 1/4	2.02 ± 2.73	ND	ND					
		Width at 1/2	8.54 ± 5.47	ND	ND					
		Width at 3/4	11.86 ± 5.15	ND	ND					
Test	rhBMP-2/ACS 1.50 mg/ml	Height	10.16 ± 4.7	ND	ND				137 ± 77	508 ± 126
		Width at 1/4	1.98 ± 2.41	ND	ND					
		Width at 1/2	7.8 ± 3.87	ND	ND					
		Width at 3/4	10.78 ± 4.63	ND	ND					
Jung et al.										
Control	Bio-Oss®	Depth	5.8 ± 1.8	5.4 ± 2.2	91 ± 15.1	13 ± 6.7	17 ± 8.1	17 ± 11.0		
		Width	ND	ND	ND					
Test	rhBMP-2/Bio-Oss®	Depth	7.0 ± 2.7	6.8 ± 0.2	96 ± 6.9	8 ± 5.0	29 ± 11.3	23 ± 11.1		
		Width	ND	ND	ND					
Anitua										
Control	—		—	—	—					
Test	PRGF (PRP)	Depth	10	ND	ND					
		Width	ND	ND	ND					
Cochran et al.										
Control	—		—	—	—					
Test	Alveolar ridge augmentation	Height	ND	−0.8 ± 2.5	ND					
		Width	ND	0.4 ± 0.9	ND					
	Socket preservation	Depth	ND	10.4 ± 6.6	ND					
		Width	ND	4.9 ± 2.4	ND					

graft group (350 ± 243 mg/cm^3) in comparison to the low (84 ± 50 mg/cm^3) and to the high (137 ± 77 mg/cm^3) dose treatment groups at 4 months after the operation. However, after 6 months of functional loading, the density of the newly induced bone increased significantly for the low (456 ± 131 mg/cm^3) and the high (508 ± 126 mg/cm^3) dose treatment groups, and its value was comparable to that of the bone graft group (448 ± 213 mg/cm^3). Jung et al. reported a positive, but not statistically significant, effect of rhBMP-2 on the amount of newly formed bone (37 ± 11.2%) in comparison to the control group (30 ± 8.9%). However, a statistically significant increase in mature lamellar bone (29 ± 11.3%) for the test site was found in comparison to the control site (17 ± 8.1%).

Safety

From the various studies, Boyne et al. [14] and Cochran et al. [17] reported the adverse events of the rhBMP-2 application that occurred during the procedure (Table 4). The most frequent adverse events occurred during the first 4 months after the operation. These events were transient and consistent with the surgical procedures performed (a maxillary sinus floor augmentation procedure, or a bone graft harvest procedure). The majority of the events were equally distributed among the treatment groups. However, the incidence of edema, rash and pain in the bone graft group were much higher than in the rhBMP-2 groups. These complaints of edema, rash (erythema), and pain were experienced from the autograft harvest site. Notably, the 1.50 mg/ml rhBMP-2/ACS treatment group had significantly greater facial edema during the first 4 months after surgery than did the bone graft group and the 0.75 mg/ml rhBMP-2/ACS group.

Discussion

This systematic review assessed the potential benefits of growth factors for bone augmentation prior to the placement of dental implants. The rhBMP-2 (INFUSE®, Medtronic) and the rhPDGF (GEM21S®, BioMinetic Therapeutics) have been approved by the FDA for dentistry. In addition, the rhBMP-7 (OP-1, Stryker Biotech) has been approved in Australia and Europe, and by the orthopedic community in the USA. Various growth factors are now entering clinical practice in dentistry. Hence, a systematic assessment of the effect of the growth factors on the bone augmentation for dental implants is very important.

The number of satisfactory studies was assumed to be low; therefore, in this systematic review with the prospective cohort studies and case reports, a lower level of evidence was used. Instead of performing a formal quality assessment of the included studies and a sensitivity analysis, this review used stringent inclusion criteria. The electronic search selected the studies, that used growth factors for bone augmentation prior to the placement of dental implants in human, by applying the following MeSH terms: "Dental Implant" and "Intercellular Signaling Peptides and Proteins". The term, "Intercellular Signaling Peptides and Proteins", belongs to the chemical and drug category, and is located at the upper level of the MeSH tree that contained all the growth factors. However, only seven studies of the

Table 4 Number of frequent adverse experiences according to the body system.

Study	Group	Body as a whole						Digestive system			
		Dehiscene	Edema	Face edema	Headache	Pain	Infection	Mouth pain	Oral edema	Oral erythema	Colitis
Boyne et al. (n = number of patient)	Bone graft (n = 13)	2	6	5	0	5	ND	8	8	6	ND
	rhBMP-2/ACS 0.75 mg/ml (n = 18)	2	0	7	2	1	ND	14	10	3	ND
	rhBMP-2/ACS 1.50 mg/ml (n = 17)	1	0	14	3	3	ND	15	8	4	ND
Cochran et al. (n = number of event)	Alveolar ridge augmentation (n = 532)	ND	ND	ND	ND	ND	1	6	1	ND	2
	Socket preservation (n = 528)	ND	ND	ND	ND	ND	1	4	2	ND	0

rhBMP-2, the rhPDGF, and the PRGF were available for an analysis. Two human RCTs for rhBMP-2 were found, but for rhPDGF and PRGF no human RCT was found. Almost all the articles were old, and no RCT evaluation of the effect of the growth factors for the dental implants had been published recently. Seven eligible articles demonstrated that the application of growth factors was safe and effective for bone formation.

Three articles related to rhBMP-2, includes this systematic review, showed a positive effect on the rhBMP application for bone formation. Cochran et al. reported a prospective, human clinical trial without a control in order to examine the effect and safety of rhBMP-2/ACS on the alveolar ridge augmentation and on the socket preservation. This study showed that bone formation was successful when using rhBMP-2/ACS at a concentration of 0.43 mg/ml. Jung et al. reported a prospective, controlled, randomized, double-masked clinical study on alveolar ridge augmentation. This study was designed to investigate the test site and the control site of the same patient's jaw, which required a lateral ridge augmentation. Despite the small number of patients, this experimental design allows the direct comparison of the test site and the control site by eliminating the differences such as the patients and the doctors or other possible variables. In addition, this is the only report that tested rhBMP-2 with grafting material (xenogenic bone substitute; Bio-Oss^{R}) for lateral bone augmentation. The report concluded that the combination of Bio-Oss^{R} with the rhBMP-2 was able to enhance the maturation process of bone regeneration and increase the graft-to-bone contact in humans. The most recent RCT study was reported by Boyne et al., and it was designed to evaluate the effect of two different concentrations of BMP-2 on the safety and efficacy of the sinus floor augmentation. It was demonstrated that the higher dosage produced better results. Based on the data, they concluded the following: (1) both the high (1.50 mg/ml) and the low (0.75 mg/ml) concentrations of rhBMP-2 were safe, with a safety profile similar to that of bone graft; (2) both concentrations of rhBMP-2 induced a similar amount of bone formation which was similar to that induced by the bone graft; and (3) the higher concentration of rhBMP-2 induced bone formation more rapidly in comparison to the lower concentration. The results support the use of rhBMP-2/ACS at a concentration of 1.50 mg/ml for the future studies of maxillary sinus floor augmentation. In these studies, the most frequent adverse events occurred within the first 4 post-operative months [14,17]. The majority of the events were equally distributed among the treatment groups and control groups. However, the high (1.50 mg/ml) concentration of rhBMP-2 treatment group had a significantly greater facial edema during the first 4 months after surgery in comparison to the bone graft group and the 0.75 mg/ml rhBMP-2/ACS group. On the other hand, we could not obtain a clear outcome from the three case reports that evaluated the rhPDGF efficacy and that met our inclusion criteria. However, the results of every study were consistent with respect to the positive effect of rhPDGF. In addition, there is no well-designed RCT study of rhPDGF. Therefore, the information was not sufficient to draw any definitive conclusions, particularly with respect to the long-term evaluation.

In addition to this systematic review, we also obtained another six eligible articles [31—36] by means of a hand-search of the articles listed in the retrieved list of References. These studies assessed — only the bone grafts. They were most likely automatically excluded on the PubMed during our selection process because the word "Dental Implant" was not associated strongly with these articles. The first studies were clinical trials, one of which was a multicenter cohort study of the effect of rhBMP-2 maxillary sinus floor augmentation and socket preservation [31,32] that supports the beneficial effect of BMPs. Fiorellini reported a randomized, masked, placebo-controlled multi-center clinical study to evaluate the effect of two concentrations of rhBMP-2 on the safety and efficacy of socket preservation [33]. The trend of this study was the same as that of the Boyne's study; 1.5 mg/ml of rhBMP-2 was safe for clinical application and the higher dosage produced better results. Van den Bergh et al. [34] and Groeneveld et al. [35] have used rhBMP-7 as an aid to increase the bone height in sinus, prior to the placement of implants. The results from these clinical trials indicated that the OP-1 (2.5 mg in 1 g of collagen carrier) had the potential to initiate bone formation in the human maxillary sinus within 6 months after a sinus floor elevation operation. However, the behavior of this material cannot be fully predicted.

Dickinson et al. [36] reported about the economic result of the rhBMP-2 treatment on the alveolar bone grafting in the older cleft patients, in order to improve poor wound healing, graft exposure, recurrent fistula, and failure of tooth eruption. According to the report for the autogenous bone graft group, seven of the nine patients underwent the procedure on an outpatient basis. The procedure was applied to the iliac bone graft patients on an inpatient basis. The donor-site pain intensity and the frequency were significant in the traditional iliac bone graft, but it was not significant in the rhBMP-2 treated group. Furthermore, the mean length of stay was greater for the iliac bone graft patients at 1.8 ± 0.8 days in comparison to the patients treated with rhBMP-2 at 0.4 ± 0.4 days ($p < 0.05$). Hence, the mean overall cost of the procedure, including the surgeon, the facility, the equipment, and the anesthesia fees, was greater for the iliac bone graft group ($21,800) in comparison to the rhBMP-2 treated group ($11,100).

On the other hand, the price of those growth factors is still relatively costly for treatment. The price of INFUSE^{R} kit which contains 4.9 mg of rhBMP-2 cost more than $3000 in the United States. The rhBMP-2 and the rhBMP-7 have been used in orthopedic spinal surgery with decreased donor-site morbidity. In addition, these proteins showed promise for the tissues that are characterized by poor wound healing, such as irradiated tissue [37]. However, there are several reports on the side effects associated with the high BMPs dosage and the repeated regimens, which are required for the stable bone regeneration in the orthopedic field [38—40]. As shown here, the use of growth factors in humans undergoing craniofacial and oral maxillofacial procedures has only recently been documented. There have been investigative reports of ectopic bone growth with rhBMP-2 and, consequently, its use in growing patients is being studied carefully [41]. In order to overcome some of these difficulties, a variety of pre-clinical studies are carried out; such as testing new optimized carrier systems to decrease the dosage of growth factors, producing the growth factors by using E-coli system [42,43], or finding the new bioactive small peptide which have osseoinduction

ability [44] to reduce the production costs and developing a genetically engineered mutant growth factors to improve the binding property to the extracellular matrix in order to prevent rapid diffusion.

BMPs have been shown to increase the formation of bone nodules *in vitro* [45—56] and stimulate bone formation *in vivo*. But the dosage applied in these clinical studies was several orders of magnitude higher than the concentration of naturally occurring BMPs [57]. It is believed that small animals require a much lower dose of BMPs to bridge bone defects in comparison to larger animals, although this correlation is expected to change appropriately for specific carriers [58]. Hydroxyapatite, natural bone mineral, collagen, gelatin hydrogels and other biodegradable polymers compose the range of carriers that are currently being investigated as vehicles for the implantation of osteogenic factors. More recently, the attention of researchers in the biomaterial field was directed at the relationship between tissue engineering and bone morphogenesis. The fundamental principle governing these investigations is the production of more "intelligent" materials that could influence protein pharmacokinetics to modulate the delivery of rhBMP-2 at the site of implantation, or to enhance osteogenesis with these factors by altering the geometry of the environment [59—62].

Recently several groups have developed genetically modified mutant rhBMP-2, which is generated from *E-coli*, and this rhBMP-2 possesses an improved binding property to the extracellular matrix in order to prevent its rapid diffusion [42,43]. Wurzler et al. reported a genetically engineered mutant rhBMP-2 (rhBMP-2 T4), which was developed with two additional repeats of a positively charged epitope, called the heparin-binding domain, in the N-terminal sequence. Bing et al. reported a genetically engineered collagen targeting rhBMP-2 (rhBMP-2-v), which was fused with collagen bonding peptide to the N-terminal of rhBMP-2. Their rhBMP-2-v contained a collagen-binding domain which modified from von Willebrand factor, and this collagen-binding domain was flanked by linker regions to minimize steric hindrance. Both genetically engineered mutant rhBMP-2 have been shown to have higher extracellular matrix binding and stronger osteoinductivity than the wild-type rhBMP-2 *in vitro* and *in vivo*. By concentrating at the targeted wound site, these BMP-2 mutants can be avoids being washed away by extracellular fluids, which will eventually lead to not only a more effective osteogenesis but also a reduction of the undesirable systemic side effects.

Therefore, many questions must be answered before the growth factors can attain widespread clinical usage. Knowledge of the cellular and molecular basis of the bone regenerative signaling pathways, and the development of appropriate carriers will certainly stimulate a great revolution in dentistry, thus allowing the dominance of regenerative over cicatricial processes. However, the number of well-designed blind and randomized clinical trials is still too small to establish the clinical protocols for the improvement of a recipient bone bed prior to implant placement, or to enhance the integration process of an implant. The dissimilarities in the experimental designs, as well as, the use of nonstandardized concentration of growth factors, or the type of carriers of growth factors by different authors make it difficult to compare the outcomes of the growth factor applications in implant dentistry. A better-designed RCT,

using growth factors for intra-oral bone augmentation, especially longitudinal clinical studies with a wider patient population, is necessary. However, these studies in this paper will set a golden standard for examining the effect of following new therapeutics.

Acknowledgment

References

[1] DeLustro F, Dasch J, Keefe J, Ellingsworth L. Immune responses to allogeneic and xenogeneic implants of collagen and collagen derivatives. Clin Orthop 1990;260:263—79.

[2] Buck BE, Malinin TI, Brown MD. Bone transplantation and human immunodeficiency virus. An estimate of risk of acquired immunodeficiency syndrome (AIDS). Clin Orthop 1989;240: 129—36.

[3] Buck BE, Resnick L, Shah SM, Malinin TI. Human immunodeficiency virus cultured from bone. Implications for transplantations. Clin Orthop 1990;251:249—53.

[4] Bessho K, Carnes DL, Cavin R, Chen HY, Ong JL. BMP stimulation of bone response adjacent to titanium implants in vivo. Clin Oral Implants Res 1999;10:212—8.

[5] Xiang W, Baolin L, Yan J, Yang X. The effect of bone morphogenetic protein on osseointegration of titanium implants. J Oral Maxillofac Surg 1993;51:647—51.

[6] Cochran DL, Nummikoski PV, Jones AA, Makins R, Turek TJ, Buser D. Radiographic analysis of regenerated bone around endosseous implants in the canine using recombinant human bone morphogenetic protein-2. Int J Oral Maxillofac Implants 1997;12:739—48.

[7] Cochran DL, Schenk R, Buser D, Wozney JM, Jones AA. Recombinant human bone morphogenetic protein-2 stimulation of bone formation around endosseous dental implants. J Periodontol 1999;70:139—50.

[8] Nevins M, Camelo M, Nevins ML, Schenk RK, Lynch SE. Periodontal regeneration in humans using recombinant human platelet-derived growth factor-BB (rhPDGF-BB) and allogenic bone. J Periodontol 2003;74:1282—92.

[9] Camelo M, Nevins ML, Schenk RK, Lynch SE, Nevins M. Periodontal regeneration in human Class II furcations using purified recombinant human platelet-derived growth factor-BB (rhPDGF-BB) with bone allograft. Int J Periodontics Restorative Dent 2003;23:213—25.

[10] Nevins M, Giannobile WV, McGuire MK, Kao RT, Mellonig JT, Hinrichs JE, et al. Platelet-derived growth factor stimulates bone fill and rate of attachment level gain: results of a large multicenter randomized controlled trial. J Periodontol 2005;76:2205—15.

[11] Simion M, Rocchietta I, Monforte M, Maschera E. Three-dimensional alveolar bone reconstruction with a combination of recombinant human platelet-derived growth factor BB and guided bone regeneration: a case report. Int J Periodontics Restorative Dent 2008;28:239—43.

[12] Byun HY, Wang HL. Sandwich bone augmentation using recombinant human platelet-derived growth facto rand beta-tricalcium phosphate alloplast: case report. Int J Periodontics Restorative Dent 2008;28:83—7.

[13] Fagan MC, Miller RE, Lynch SE, Kao RT. Simultaneous augmentation of hard and soft tissues for implant site preparation using recombinant human platelet-derived growth factor: a human case report. Int J Periodontics Restorative Dent 2008;28:37—43.

[14] Boyne PJ, Lilly LC, Marx RE, Moy PK, Nevins M, Spagnoli DB, et al. De novo bone induction by recombinant human bone morphogenetic protein-2 (rhBMP-2) in maxillary sinus floor augmentation. J Oral Maxillofac Surg 2005;63:1693–707.

[15] Jung RE, Glauser R, Scharer P, Hammerle CH, Sailer HF, Weber FE. Effect of rhBMP-2 on guided bone regeneration in humans. Clin Oral Implants Res 2003;14:556–68.

[16] Anitua E. The use of plasma-rich growth factors (PRGF) in oral surgery. Pract Proced Aesthet Dent 2001;13:487–93.

[17] Cochran DL, Jones AA, Lilly LC, Fiorellini JP, Howell H. Evaluation of recombinant human bone morphogenetic protein-2 in oral applications including the use of endosseous implants: 3-year results of a pilot study in humans. J Periodontol 2000;71:1241–57.

[18] Anitua E, Orive G, Aguirre JJ, Andía I. Clinical outcome of immediately loaded dental implants bioactivated with plasma rich in growth factors: a 5-year retrospective study. J Periodontol 2008;79:1168–76.

[19] Lynch SE, Wisner-Lynch L, Nevins M, Nevins ML. A new era in periodontal and periimplant regeneration: use of growth-factor enhanced matrices incorporating rhPDGF. Compend Contin Educ Dent 2006;27:672–8.

[20] Block MS, Achong R. Bone morphogenetic protein for sinus augmentation. Atlas Oral Maxillofac Surg Clin N Am 2006;14:99–105.

[21] Block MS, Jackson WC. Techniques for grafting the extraction site in preparation for dental implant placement. Atlas Oral Maxillofac Surg Clin N Am 2006;14:1–25.

[22] Wikesjo UM, Polimeni G, Qahash M. Tissue engineering with recombinant human bone morphogenetic protein-2 for alveolar augmentation and oral implant osseointegration: experimental observations and clinical perspectives. Clin Implant Dent Relat Res 2005;7:112–9.

[23] Garg AK, Gargenese D, Peace I. Using platelet-rich plasma to develop an autologous membrane for growth factor delivery in dental implant therapy. Dent Implantol Update 2000;11:41–4.

[24] Simon Z, Watson PA. Biomimetic dental implants-new ways to enhance osseointegration. J Can Dent Assoc 2002;68:286–8.

[25] Garg AK. The use of platelet-rich plasma to enhance the success of bone grafts around dental implants. Dent Implantol Update 2000;11:17–21.

[26] Salata LA, Franke-Stenport V, Rasmusson L. Recent outcomes and perspectives of the application of bone morphogenetic proteins in implant dentistry. Clin Implant Dent Relat Res 2002;4:27–32.

[27] Growth factors and their potential use in bone grafting procedures for dental implants. Dent Implantol Update 2002;13:1–5.

[28] Rose LF, Rosenberg E. Bone grafts and growth and differentiation factors for regenerative therapy: a review. Pract Proced Aesthet Dent 2001;13:725–34.

[29] Becker W, Clokie C, Sennerby L, Urist MR, Becker BE. Histologic findings after implantation and evaluation of different grafting materials and titanium micro screws into extraction sockets: case reports. J Periodontol 1998;69:414–21.

[30] Koka S, Vance JB, Maze GI. Bone growth factors: potential for use as an osseointegration enhancement technique (OET). J West Soc Periodontol Periodontal Abstr 1995;43:97–104.

[31] Howell TH, Fiorellini J, Jones A, Alder M, Nummikoski P, Lazaro M, et al. A feasibility study evaluating rhBMP-2/absorbable collagen sponge device for local alveolar ridge preservation or augmentation. Int J Periodontics Restorative Dent 1997;17:124–39.

[32] Boyne PJ, Marx RE, Nevins M, Triplett G, Lazaro E, Lilly LC, et al. A feasibility study evaluating rhBMP-2/absorbable collagen sponge for maxillary sinus floor augmentation. Int J Periodontics Restorative Dent 1997;17:11–25.

[33] Fiorellini JP, Howell TH, Cochran D, Malmquist J, Lilly LC, Spagnoli D, et al. Randomized study evaluating recombinant human bone morphogenetic protein-2 for extraction socket augmentation. J Periodontol 2005;76:605–13.

[34] van den Bergh JP, ten Bruggenkate CM, Groeneveld HH, Burger EH, Tuinzing DB. Human segmental mandibular defects treated with naturally derived bone morphogenetic proteins. J Clin Periodontol 2000;27:627–36.

[35] Groeneveld EH, van den Bergh JP, Holzmann P, ten Bruggenkate CM, Tuinzing DB, Burger EH. Histomorphometrical analysis of bone formed in human maxillary sinus floor elevations grafted with OP-1 device, demineralized bone matrix or autogenous bone. Comparison with non-grafted sites in a series of case reports. Clin Oral Implants Res 1999;10:499–509.

[36] Dickinson BP, Ashley RK, Wasson KL, O'Hara C, Gabbay J, Heller JB, et al. Reduced morbidity and improved healing with bone morphogenic protein-2 in older patients with alveolar cleft defects. Plast Reconstr Surg 2008;121:209–17.

[37] Howard BK, Brown KR, Leach JL, Chang CH, Rosenthal DI. Osteoinduction using bone morphogenic protein in irradiated tissue. Arch Otolaryngol Head Neck Surg 1998;124:985–8.

[38] Benglis D, Wang MY, Levi AD. A comprehensive review of the safety profile of bone morphogenetic protein in spine surgery. Neurosurgery 2008;62:423–31.

[39] Vaibhav B, Nilesh P, Vikram S, Anshul C. Bone morphogenic protein and its application in trauma cases: a current concept. Injury 2007;38(11):1227–35.

[40] Hwang CJ, Vaccaro AR, Lawrence JP, Hong J, Schellekens H, Alaoui-Ismaili MH, et al. Immunogenicity of bone morphogenetic proteins. J Neurosurg Spine 2009;10(5):443–51.

[41] Wong DA, Kumar A, Jatana S, Ghiselli G, Wong K. Neurologic impairment from ectopic bone in the lumbar canal: a potential complication of off-label PLIF/TLIF use of bone morphogenetic protein-2 (BMP-2). Spine J 2008;8:1011–8.

[42] Wurzler KK, Emmert J, Eichelsbacher F, Kubler NR, Sebald W, Reuther JF. Evaluation of the osteoinductive potential of genetically modified BMP-2 variants. Mund Kiefer Gesichtschir 2004;82:83–92.

[43] Chen B, Lin H, Zhao Y, Wang B, Zhao Y, Liu Y, et al. Activation of demineralized bone matrix by genetically engineered human bone morphogenetic protein-2 with a collagen binding domain derived from von Willebrand factor propolypeptide. J Biomed Mater Res A 2007;80(2):428–34.

[44] Egusa H, Kaneda Y, Akashi Y, Hamada Y, Matsumoto T, Saeki M, et al. Enhanced bone regeneration via multimodal actions of synthetic peptide SVVYGLR on osteoprogenitors and osteoclasts. Biomaterials 2009;30(27):4676–86.

[45] Zhang H, Sucato DJ, Welch RD. Recombinant human bone morphogenic protein-2-enhanced anterior spine fusion without bone encroachment into the spinal canal: a histomorphometric study in a thoracoscopically instrumented porcine model. Spine 2005;30:512–8.

[46] Ashinoff RL, Cetrulo CL, Galiano RD, Dobryansky M, Bhatt KA, Ceradini DJ, et al. Bone morphogenic protein-2 gene therapy for mandibular distraction osteogenesis. Ann Plast Surg 2004;52:585–90.

[47] Rachmiel A, Aizenbud D, Peled M. Enhancement of bone formation by bone morphogenetic protein-2 during alveolar distraction: an experimental study in sheep. J Periodontol 2004;75:1524–31.

[48] Mayer M, Hollinger J, Ron E, Wozney J. Maxillary alveolar cleft repair in dogs using recombinant human bone morphogenetic protein-2 and a polymer carrier. Plast Reconstr Surg 1996;98:247–59.

[49] Valentin-Opran A, Wozney J, Csimma C, Lilly L, Riedel GE. Clinical evaluation of recombinant human bone morphogenetic protein-2. Clin Orthop Relat Res 2002;395:110–20.

[50] Miranda DA, Blumenthal NM, Sorensen RG, Wozney JM, Wikesjö UM. Evaluation of recombinant human bone morphogenetic

protein-2 on the repair of alveolar ridge defects in baboons. J Periodontol 2005;76:210—20.

[51] Wikesjo UM, Sorensen RG, Kinoshita A, Jian Li X, Wozney JM. Periodontal repair in dogs: effect of recombinant human bone morphogenetic protein-12 (rhBMP-12) on regeneration of alveolar bone and periodontal attachment. J Clin Periodontal 2004;31:662—70.

[52] Farhadieh RD, Gianoutsos MP, Yu Y, Walsh WR. The role of bone morphogenetic proteins BMP-2 and BMP-4 and their related postreceptor signaling system (Smads) in distraction osteogenesis of the mandible. J Craniofac Surg 2004;15:714—8.

[53] Jovanovic SA, Hunt DR, Bernard GW, Spiekermann H, Nishimura R, Wozney JM, et al. Long-term functional loading of dental implants in rhBMP-2 induced bone: a histologic study in the canine ridge augmentation model. Clin Oral Implants Res 2003;14:793—803.

[54] Kitamura A, Motohashi N, Kawamoto T, Baba Y, Suzuki S, Kuroda T. Tooth eruption into the newly generated bone induced by recombinant human bone morphogenetic protein-2. Cleft Palate Craniofac J 2002;39:449—56.

[55] Nagao H, Tachikawa N, Miki T, Oda M, Mori M, Takahashi K, et al. Effect of recombinant human bone morphogenetic protein-2 on bone formation in alveolar ridge defects in dogs. Int J Oral Maxillofac Surg 2002;31:66—72.

[56] Choi SH, Kim CK, Cho KS, Huh JS, Sorensen RG, Wozney JM, et al. Effect of recombinant human bone morphogenetic protein-2/absorbable collagen sponge (rhBMP-2/ACS) on healing in 3-wall intrabony defects in dogs. J Periodontol 2002;73:63—72.

[57] Urist MR, DeLange RJ, Finerman GAM. Bone cell differentiation and growth factors: induced activity of chondro-osteogenic DNA. Science 1983;220:680—5.

[58] Seeherman H. The influence of delivery vehicles and their properties on the repair of segmental defects and fractures with osteogenic factors. J Bone Joint Surg Am 2001;83:79—81.

[59] Yoshida K, Bessho K, Fujimura K. Enhancement by recombinant human bone morphogenetic protein-2 of bone formation by means of porous hydroxyapatite in mandibular bone defect. J Dent Res 1999;78:1505—10.

[60] Kuboki Y, Jin Q, Takita H. Geometry of carriers controlling phenotypic expression in rhBMP-induced osteogenesis and chondrogenesis. J Bone Joint Surg Am 2001;83:105—15.

[61] Ripamonti U, Crooks J, Rueger DC. Induction of bone formation by recombinant human osteogenic protein-1 and sintered porous hydroxyapatite in adult primates. Plast Reconstr Surg 2001;107:977—88.

[62] Uludag H, Gao T, Porter TJ, Friess W, Wozney JM. Delivery system for BMPs; factors contributing to protein retention at an application site. J Bone Joint Surg Am 2001;83:128—35.

Real time assessment of surface interactions with a titanium passivation layer by surface plasmon resonance

Isao Hirata [a,*], Yasuhiro Yoshida [b], Noriyuki Nagaoka [b], Kyou Hiasa [a], Yasuhiko Abe [a], Kenji Maekawa [b], Takuo Kuboki [b], Yasumasa Akagawa [a], Kazuomi Suzuki [b], Bart Van Meerbeek [c], Phillip B. Messersmith [d], Masayuki Okazaki [a]

[a] Graduate School of Biomedical Sciences, Hiroshima University, 1-2-3 Kasumi, Minami-ku, Hiroshima 734-8553, Japan
[b] Graduate School of Medicine, Dentistry and Pharmaceutical Sciences, Okayama University, 2-5-1 Shikata-cho, Kita-ku, Okayama 700-8525, Japan
[c] Leuven BIOMAT Research Cluster, Department of Conservative Dentistry, Catholic University of Leuven, Kapucijnenvoer 7, B-3000 Leuven, Belgium
[d] Department of Biomedical Engineering, Northwestern University, 2145 Sheridan Road, Evanston, IL 60208, USA

ARTICLE INFO

ABSTRACT

Due to the high corrosion resistance and strength to density ratio titanium is widely used in industry, and also in a gamut of medical applications. Here we report for the first time on our development of a titanium passivation layer sensor that makes use of surface plasmon resonance (SPR). The deposited titanium metal layer on the sensor was passivated in air, similarly to titanium medical devices. Our "Ti-SPR sensor" enables analysis of biomolecule interactions with the passivated surface of titanium in real time. As a proof of concept, corrosion of a titanium passivation layer exposed to acid was monitored in real time. The Ti-SPR sensor can also accurately measure the time-dependence of protein adsorption onto the titanium passivation layer at sub-nanogram per square millimeter accuracy. Besides such SPR analyses, SPR imaging (SPRI) enables real time assessment of chemical surface processes that occur simultaneously at "multiple independent spots" on the Ti-SPR sensor, such as acid corrosion or adhesion of cells. Our Ti-SPR sensor will therefore be very useful to study titanium corrosion phenomena and biomolecular titanium–surface interactions with application in a broad range of industrial and biomedical fields.

© 2011 Acta Materialia Inc. Published by Elsevier Ltd. All rights reserved.

1. Introduction

Thanks to its high strength to density, excellent corrosion resistance, decreasing cost, and increasing availability, titanium and its alloys enjoy widespread industrial applications in a wide variety of highly corrosive environments, including sea water, bleaches, alkaline solutions, oxidizing agents, and organic acids [1]. These excellent properties mean that titanium is widely used in industries including aerospace, marine, power generation, and desalination plants, for instance [2–5]. Its extremely high corrosion resistance results from the formation of a very stable, continuous, highly adherent, and protective oxide film on the titanium surface, formed spontaneously and instantly once fresh metal surfaces are exposed to air or moisture.

Titanium is also commonly used to fabricate a variety of medical devices such as hip and knee joints, bone screws and plates, dental implants, stents, pacemaker cases and centrifugal pumps in artificial hearts [6–8]. Due to rapidly aging populations, especially in developed countries, national health care costs are escalating. In particular, the increased incidence of hard tissue and cardiovascular diseases such as periodontitis, osteoarthritis, and arteriostenosis is strongly correlated with the rapidly growing elderly population. Therefore, the development of innovative treatment techniques for functional repair or complete cure of these diseases is highly desirable. In attempts to improve the healing potential of such medical device, much research has been devoted to titanium surface modification methods that enable controlled adsorption of biomolecules and ions or regulated drug release [9–12]. In biomaterial sciences the strategic importance of fundamental research in nanobiotechnology has recently been acknowledged [13]. The development of highly sensitive methods that can monitor the interaction of biomolecules at titanium surfaces are therefore needed.

Surface plasmon resonance (SPR) can offer real time and label-free analysis of the interfacial events that occur on the surface of a metal layer under physiological conditions [14,15]. Recently, the technique of SPR imaging (SPRI) has been developed and applied to monitor the adsorption of organic materials and biomolecules at multiple independent spots [16]. In this study we report for the first time on our development of a titanium passivation surface sensor chip for SPR [17]. There are few reports of titanium SPR (Ti-SPR) sensors in which the titanium metal layer was passivated

* Corresponding author. Fax: +81 82 257 5649.
  E-mail address: isao@hiroshima-u.ac.jp (I. Hirata).

in air. Although many studies of a TiO$_2$-coated sensor for SPR have been reported [18–23], their sensors were directly coated with TiO$_2$ and titanium metal was not used. In medicine and dentistry the titanium metal surface of dental implants and artificial bones oxidize in air. Our Ti-SPR sensor has a titanium passivation layer, closely resembling the conditions under which titanium medical devices are normally used during clinical treatment.

2. Experimental section

2.1. Materials

Bovine serum albumin was purchased from Sigma–Aldrich Japan K.K. (Tokyo, Japan). γ-Globulin was purchased from Nacalai Tesque Inc. (Kyoto, Japan). bFGF (recombinant human basic growth factor, KCB-1) was kindly donated by Kaken Pharmaceutical Co. Ltd. (Kyoto, Japan). Dulbecco's phosphate buffered saline without calcium and magnesium (pH 7.4) (PBS) was purchased from Nissui Pharmaceutial Co. Ltd. (Tokyo, Japan). Dodecylphosphate (DDP) was purchased from Alfa Aesar (Ward Hill, MA). Other chemicals were purchased from Wako Pure Chemical Industries (Osaka, Japan). All chemicals were used as received without any additional purification. Glass plates made of S-LAL10 (refractive index 1.72, diameter 15 mm, thickness 1 mm) were purchased from Arteglass Associates Co. (Kyoto, Japan).

2.2. Surface plasmon resonance instruments

We constructed a SPR instrument which determines the SPR spectrum and the SPR angle shift [24,25]. The SPR instrument, constructed with reference to Knoll's method, utilized the Kretschmann configuration in which the metal was in the form of a thin film mounted directly onto a S-LAL10 glass plate coupled to an S-LAL10 dispersing prism with an index matching fluid [14,26]. An SPR chip was attached to the SPR flow cell, which was 10 mm in length, 1 mm in width, and 1 mm in thickness. Solutions were allowed to pass through the flow cell [25]. The He–Ne laser light (λ = 632.8 nm) was linearly p-polarized using a Gran–Thomson prism and then passed through a non-polarizing cube beam splitter. The sample surface was exposed to the p-polarized light through the prism. The intensity of the reflected light was determined by a photodiode detector. A computer was used to control a biaxial rotation stage and to process the intensities of the incident and reflected light as a SPR spectrum. At the angle at which there is a dip in the spectrum the light resonated surface plasmons on the metal layer. This angle is called the SPR angle [14,15].

The SPR-1000 SPRI apparatus (UBM, Kyoto, Japan) employed in this study was developed with reference to our SPRI apparatus [16]. The SPR chip with arrayed spots was mounted on an S-LAL10 dispersing prism with index matching fluid. The flow cell was constructed using a washer made of silicone and a vinyl chloride lid with an inlet and outlet. The back of the chip was illuminated by p-polarized, collimated, and polychromatic white light through the prism. The reflected light was passed through an interference filter and collected by a CCD camera. The data was acquired using our in-house designed software.

The Ti-SPR sensor chip can be used in both instruments. All experiments were carried out at 25 °C.

2.3. Development and evaluation of the titanium SPR sensor

2.3.1. Design of the titanium SPR sensor

General SPR sensor chips are based on gold-coated glass substrates. The Ti-SPR sensor chips were prepared by depositing titanium metal on the contamination-free gold surface of the SPR sensor. To design an optimal Ti-SPR sensor it was necessary to consider the thickness and oxidation of the deposited titanium layer and the detection of protein adsorption in water solutions. So the SPR spectra of the Ti-SPR sensor were simulated using the Fresnel equation of reflection and transmission using a prism, glass plate, Cr, Au, Ti, TiO$_2$, protein, and water multilayer (Fig. 1) to estimate the optimal layer thickness of the deposited titanium [26,27]. When the amount of protein adsorption or the thickness of the TiO$_2$ layer is changed, the SPR angle is shifted. So the shift in the SPR angle (degree) can be calculated as the amount of protein (4.02 ng mm^{-2} degree^{-1}) or the thickness of the etched TiO$_2$ layer (0.77 nm degree^{-1}).

The designed Ti-SPR sensor chips were prepared by Osaka Vacuum Industrial Co. Ltd. (Osaka, Japan). These chips were prepared by depositing Cr, Au, and Ti on S-LAL10 glass plates under 2.0×10^{-2} Pa using an electron beam evaporation method.

2.3.2. Characterization of the titanium layer on the Ti-SPR sensor

A transmission electron microscopy (TEM) cross-section of the developed Ti-SPR sensor chip embedded in epoxy resin was prepared using an Ion Slicer (EM-09100IS, JEOL), and imaged using a JEM-3010 (JEOL) microscope operated at 300 keV. The surface elemental composition of the Ti-SPR sensor was determined using X-ray photoelectron spectroscopy (XPS) (AXIS-HS, Kratos, Manchester, UK) in vacuo at less than 10^{-7} Pa. We used AlK$_\alpha$ monochromatic X-rays with a source power of 150 W (acceleration voltage of 15 kV and filament current of 10 mA) and measured the elemental composition ratio of Au, Ti, and O at photo-electron take-off angles of 90°, 60°, 45°, 30°, and 15°. The layer thicknesses of the titanium and the oxidized titanium on the Ti-SPR sensor were estimated from the SPR spectrum of this sensor and the relationship between the amount of protein adsorbed and the SPR angle shift was determined.

2.4. SPR measurements of acid etching and biomolecule adsorption

2.4.1. Effect of acid etching on the titanium surface

The effect of acid etching the titanium surface was determined by SPR. Phosphoric acid solutions were prepared by dropping 85 wt.% phosphoric acid into pure water to obtain pH values of 1.8, 1.9, 2.0, and 3.0. The running solution used was pure water.
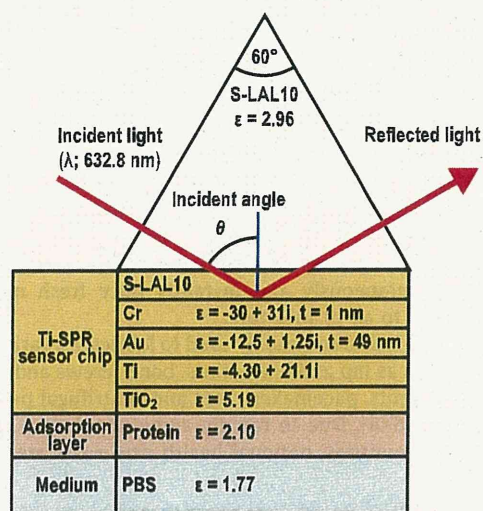

Fig. 1. Schematic illustrating the Ti-SPR sensor with the coupled prism for SPR. The deposited titanium metal layer is easily oxidized by air and its thickness changed. The thickness and dielectric constant are indicated for each coated/adsorbed substance (S-LAL10 glass, Cr, Au, Ti, TiO$_2$, protein, and PBS).

The Ti-SPR sensor chip was attached to an SPR flow cell. Pure water was allowed to pass through the flow cell until the SPR angle was stable. The SPR spectrum for the Ti-SPR sensor exposed to pure water was recorded and then the incident light angle was fixed at 1.0° lower than the minimum of reflectance, which was the SPR angle. Subsequently the intensity of the reflected light was followed during exposure to phosphoric acid solution flow for 20 min. Then this solution was washed out with water for 19 min and the SPR spectrum again recorded. The SPR angle shift was determined from the minima of the two resonance profiles.

The effect of acid etching the titanium was also determined using a quartz crystal micro-balance (QCM) (Q-Sense D300). A QSX 310 (titanium QCM sensor) was attached to a QCM flow cell (QWiC301). All QCM apparatus and chips were purchased from Q-Sense AB (Västra Frölunda, Sweden). Pure water was allowed to pass through the flow cell until the frequency of the quartz crystal was stable. Subsequently phosphoric acid solution was allowed to flow for 20 min. Finally, this solution was washed out of the flow cell with pure water for 19 min. The phosphoric acid solutions used were either pH 1.8 or 2.0.

All solutions flowed at 3.3 ml min^{-1} in both experiments.

2.4.2. Protein and polymer adsorption on the titanium surface

The amount of protein and polymer adsorbed onto the titanium surface was determined by the Ti-SPR sensor. The Ti-SPR sensor chip was attached to an SPR flow cell and then PBS was allowed to pass through the flow cell at 3.3 ml min^{-1}. The SPR spectrum was recorded when the SPR angle had become stable. Subsequently the intensity of the reflected light was followed during exposure to a protein or polymer solution under flow for 10 min. Then this solution was washed out with PBS for 9 min and the SPR spectrum was again recorded. The protein solutions used were 2 µg ml^{-1} albumin, γ-globulin, and bFGF in PBS. The polymer solutions used were 100 µg ml^{-1} polyethyleneimine (PEI) and gelatin in PBS, and 1 wt.% poly(phosphoric acid) (PPAc) in water.

2.5. SPRI measurements of cell response and corrosion resistance

2.5.1. Preparation of the titanium array for SPRI

The titanium surface of the Ti-SPR sensor chip was cleaned by argon plasma irradiation (electrode current of 23 mA for 90 s), and then immersed in acetone and toluene for 5 min each. This washed chip was then immersed in 2 mM octadecyltrichlorosilane (ODTCS) dissolved into toluene for 24 h at 60 °C. After silane treatment this chip was washed successively with toluene, acetone, a 1:1 (v/v) acetone–water mixture, and, finally, again with acetone. This OTDCS layer adsorbed onto the titanium surface was then irradiated/etched with argon plasma (electrode current of 10 mA for 10 min) through a stainless steel mask (5 × 5 pore arrays with a circular pore size of 1 mm, and an inter-pore interval of 1 mm) in order to produce 1 mm diameter titanium spots on the OTDCS-coated Ti-SPR sensor chip. This patterned array chip was immersed in acetone.

2.5.2. Preparation of the polymer-coated titanium array

The polymer-coated titanium array chip was prepared by dropping 1 µl of PBS onto the titanium spots of the titanium array chip, after which the chip was kept in saturated water vapor for 20 min. Then the PBS drops were removed and 0.5 µl of PEI, gelatin, PPAc, and PBS were dropped onto these spots, after which the chip was again kept in saturated water vapor for 20 min. Finally, each spot was washed five times with PBS.

2.5.3. Cells interactions with titanium assessed using SPRI

The interaction of cells with the polymer-coated titanium array chip was determined by SPRI. An albumin-free PIPES buffered medium (25 mM PIPES (pH 7.2), 159 mM NaCl, 5 mM KCl, 0.4 mM MgCl$_2$, 1 mM CaCl$_2$, 5.6 mM glucose) [28] was prepared as solvent and the sample solution used was a MC3T3-E1 cell suspension (500,000 cells in 1 ml of this medium). The chip was attached to an SPRI batch cell. 300 µl of the medium was dropped onto the batch cell and the SPRI image was allowed to stabilize. Then 100 µl of the cell suspension was dropped onto the batch cell and mixed in situ, while the SPRI image data were recorded for 1 h. Phase contrast microscopy images of cell attachment to the polymer-spotted array chip were obtained under the above conditions.

2.5.4. Preparation of the DDP-treated titanium array

The DDP-treated array chip was prepared by dropping 0.3 µl of 1 wt.% DDP dissolved in 1:1 (w/w) water–ethanol mixture onto the titanium spots of the titanium array chip, after which the chip was kept in saturated water vapor for 30 min. Then the chip was washed three times with acetone.

2.5.5. Observation of the corrosion resistance of DDP-treated titanium by SPRI

The process of acid etching the DDP-coated titanium array chip was observed by SPRI for 10 min. An HCl/KCl buffered solution (41.4 mM HCl, 50.0 mM KCl, pH 1.5) [29] and a KCl solution (63.1 mM) were prepared as the "running" and "sample" solutions, respectively. The chip was attached to an SPRI flow cell. The running solution was allowed to pass through the flow cell and the SPRI image was allowed to stabilize. Then the SPRI data were recorded simultaneously at different spots during exposure to the sample solution at a flow rate of 3.3 ml min^{-1}.

3. Results and discussion

3.1. Development of the titanium SPR sensor

To design the Ti-SPR sensor the SPR spectrum needed to be simulated. Fig. 2 shows the simulated SPR spectra in relation to the thickness and the oxidation rates of the titanium layers. The titanium layer deposited on the SPR sensor chip easily oxidizes in air (leading to increased corrosion resistance). When the titanium layer (atomic weight 47.9, density 4.5 g cm^{-3}) is oxidized to a titanium dioxide layer (molecular weight 79.9) the density is reduced and the thickness increased [30]. As the density of titanium dioxide crystals is 3.8 (antase) or 4.2 (rutile) g cm^{-3} and the oxidized titanium layer on the Ti-SPR sensor is expected to show low crystallinity and to contain many hydroxyl groups [30–32], we assumed that the density of the oxidized titanium layer was 4.0 g cm^{-3}, that it grew in the uniaxial direction and that the thickness of this layer increased 1.9 times as a result of oxidization. In the case of a 5 nm thick titanium surface layer the peak of the SPR spectrum became sharper with increasing oxidation. In case of a 10 nm titanium layer, however, the peak of the SPR spectrum did not become sharper and the SPR angle, which is a minimum reflectance angle in the SPR spectrum, occurred at a high incident light angle. The latter is disadvantageous because the amount of protein adsorbed is related to the increase in SPR angle. In the case of a 20 nm Ti layer no peak occurred in the SPR spectrum. These simulations suggest that the thinner the titanium layer is the more accurate ("sharper") the SPR spectrum is. Therefore, a Ti-SPR sensor with an optimal 5 nm thick titanium layer was employed.

3.2. Evaluation of the Ti-SPR sensor surface

The simulation was insufficient to determine the actual thickness of the surface oxide layer. So we measured the Ti-SPR sensor chip, as shown in Figs. 3 and 4, using TEM and SPR. The thinnest
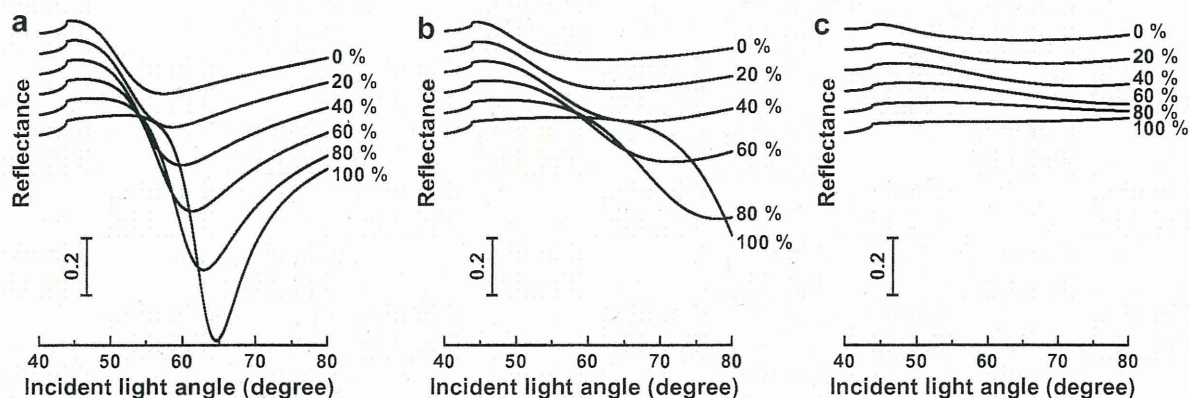
Fig. 2. Simulation of SPR spectra for 0, 20, 40, 60, 80, and 100% oxidized titanium metal layers in air. The thicknesses of the vapor deposited titanium metal layer were (a) 5, (b) 10, and (c) 20 nm.
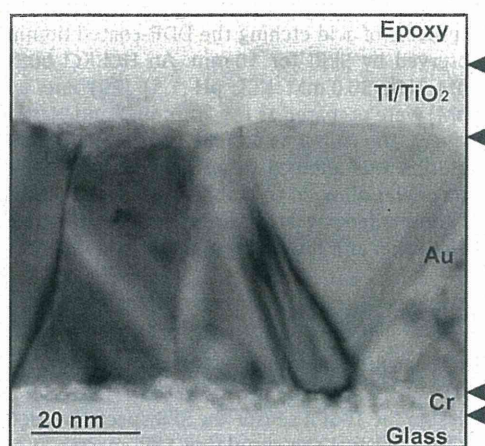

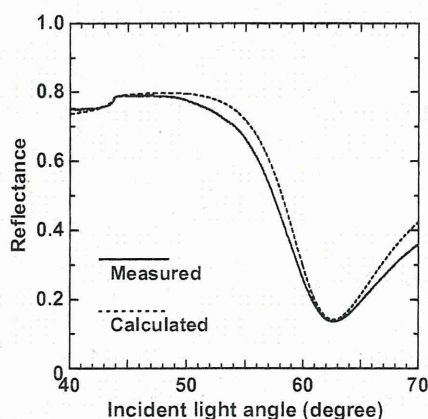**Fig. 3.** High magnification cross-sectional TEM image of the Ti-SPR sensor.

Fig. 5. Atom fraction of Au (●) and O/Ti (○) ratio on the surface of the Ti-SPR sensor as measured by angle-dependent XPS.

Fig. 4. SPR spectrum of the developed Ti-SPR sensor. A 5 nm titanium metal layer was deposited on this sensor. The continuous and dotted lines represent the measured and theoretically calculated spectra (titanium, 0.7 nm; titanium dioxide, 7.6 nm), respectively.

achievable titanium layer that could be sputter coated was 5 nm. High magnification cross-sectional TEM images of the Ti-SPR sensor (Fig. 3) showed a 49 nm Au layer with an about 10 nm Ti/TiO$_2$ layer on top and a Cr layer underneath on top of the glass substrate. The spectrum of the Ti-SPR sensor was detected in the SPR
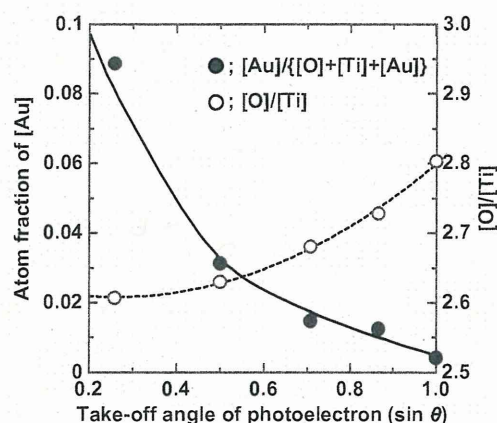
results (Fig. 4), and the thickness of the oxide layer was obtained by comparing the simulated and measured SPR spectra. The dotted line in Fig. 4 shows the simulated SPR spectrum for a 0.7 nm thick titanium layer and a 7.6 nm titanium dioxide layer. Good agreement was found with the actual and simulated SPR spectra.

Fig. 5 shows the results for the atom fraction of Au and the O/Ti ratio at the Ti-SPR sensor surface as measured by angle-dependent XPS, confirming that the gold layer was uniformly coated with an ultrathin oxidized titanium layer, and that the O/Ti ratio at the top was larger than at the bottom. The non-stoichiometric O/Ti ratio may be due to the fact that the outer surface contained titanium hydroxide (TiO(OH)$_2$ with an O/Ti ratio of 3, while the O/Ti ratio of TiO$_2$ is 2), and because the oxygen atoms in these hydroxyl groups seemed to mainly exist in the top layer. From these results it was concluded that the external layer of the titanium surface SPR sensor was titania.

3.3. Detection of acid etching on the titanium surface

Titanium is very corrosion resistant, thanks to the presence of the passivating film on the surface. When we exposed the surface of the Ti-SPR sensor to phosphoric acid solutions of different pH (Fig. 6a) the SPR angles shifted to lower values, except for the pH 3.0 solution. This indicates that the oxidized titanium surface was etched when exposed to phosphoric acid solutions with a pH of 2.0 or below. The average thickness changes at pH 2.0, 1.9, and 1.8 were about 20, 50, and 120 pm, respectively.
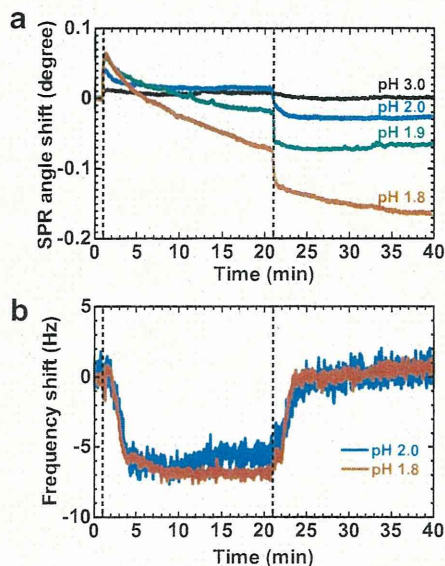
Fig. 6. Effect of etching the titanium passivation layer with phosphoric acid at different pH, as measured by (a) SPR and (b) QCM. The acid solutions were flowed for 20 min and then were washed out with pure water for 19 min.

Using QCM, the effect of etching titanium was also determined under the same conditions (Fig. 6b), but the relatively low signal-to-noise ratio obscured the QCM spectrum. Pressure fluctuations in the flow solution strongly affect the frequency of the quartz crystal, whereas the optical performance of the Ti-SPR sensor is largely unaffected under similar conditions. The Ti-SPR sensor has high sensitivity when measuring titanium etching, which is achievable because TiO_2 has a higher dielectric constant ($\varepsilon = 5.19$) than phosphoric acid ($\varepsilon = 2.12$) [33] in water and, consequently, the SPR angle shift due to changes in layer thickness is about 5 times more sensitive for TiO_2 (0.77 nm degree^{-1}) than for phosphoric acid (4 nm degree^{-1}).

The above mentioned experiments confirm the real time high resolution acid etching measuring capability of the Ti-SPR sensor.

3.4. Measurement of biomolecule adsorption on the titanium surface

Thanks to high biocompatibility, titanium is commonly used in a variety of medical devices. However, chemical and biological reactions of non-treated titanium surfaces are poor because of its chemical stability. Therefore, many methods of modifying titanium surfaces have been studied to increasing the bioactivity, bone conductivity, and biocompatibility [32,34,35].

In this study the Ti-SPR sensor was used to measure the interaction between biomolecules and the titanium passivation layer in real time. Fig. 7 shows increasing protein absorption on Ti with time for the three proteins studied. It was assumed that the difference in pI and molecular weight of the proteins would influence the amount of protein absorbed. At pH 7.4 the Ti surface is negatively charged [36], γ-globulin is slightly negatively charged, albumin is negatively charged, and bFGF is positively charged. Therefore, we hypothesized that γ-globulin (158 kDa, pI 5.8–7.3) would be most adsorbed on Ti (2.85 ng mm^{-2}) because of its greater molecular weight, albumin (69 kDa, pI 4.9) would be least adsorbed (0.85 ng mm^{-2}) because of its negative charge, and bFGF (17 kDa, pI 10.1), although having a molecular weight 10 times less than that of γ-globulin, was adsorbed to a greater extent (2.08 ng mm^{-2}) than albumin because of its positive charge.

The Ti-SPR sensor also enabled us to measure changes in adsorption of polymers to surfaces such as, for instance, titanium
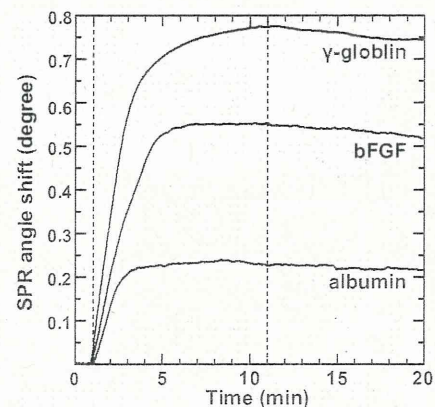

Fig. 7. Time evolution of protein adsorption on the titanium passivation layer by SPR. Protein solutions in PBS were 2 μg ml^{-1} γ-globulin, 2 μg ml^{-1} albumin, and 2 μg ml^{-1} bFGF. The protein solutions were flowed for 10 min and then were washed out with PBS for 9 min.

medical devices coated with different polymers in order to achieve slow release of drugs and cytokines [37]. Real time changes in the SPR angle were measured when titanium was exposed to PEI, gelatin, and PPAc suspensions (Fig. 8). While PEI and gelatin were rapidly adsorbed onto the titanium surface and resisted removal by washing, PPAc significantly etched the surface due to its low pH (pH 1.5), but deposited a thin PPAc layer upon washing [38].

These results indicate that the Ti-SPR sensor developed can accurately measure time-dependent protein and polymer adsorption onto a titanium passivation layer.

3.5. SPRI observation of cell response on the titanium surface

A variant of the sensor enables SPRI mapping of biological surface processes. Using SPRI the cell response on a polymer-coated titanium array chip could be studied in real time (Fig. 9a and b). The response of MC3T3-E1 cells was found to increase on the spots coated with PPAc, titanium, PEI, and gelatin, in that order. Unfortunately, the cell response on the surface reflects not only cell adhesives but also cell reactions [39]. This differential cell adhesion was confirmed by phase contrast microscopy (Fig. 9c), which showed that cells adherent on the PPAc spot and the gelatin spot developed filopodia along with spread cell bodies, while cells on the PEI spot
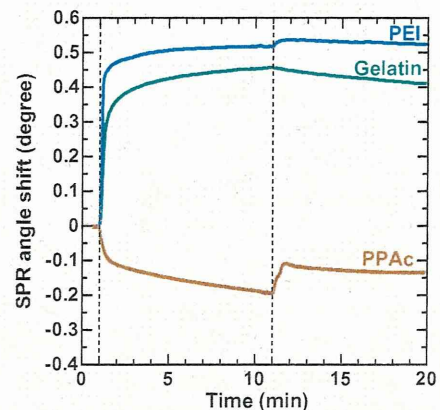

Fig. 8. Time evolution of polymer adsorption on the titanium passivation layer by SPR. Polymer solutions were 100 μg ml^{-1} PEI and 100 μg ml^{-1} gelatin in PBS, and 1 wt.% PPAc in water. The polymer solutions were flowed for 10 min and then were washed out with PBS for 9 min.
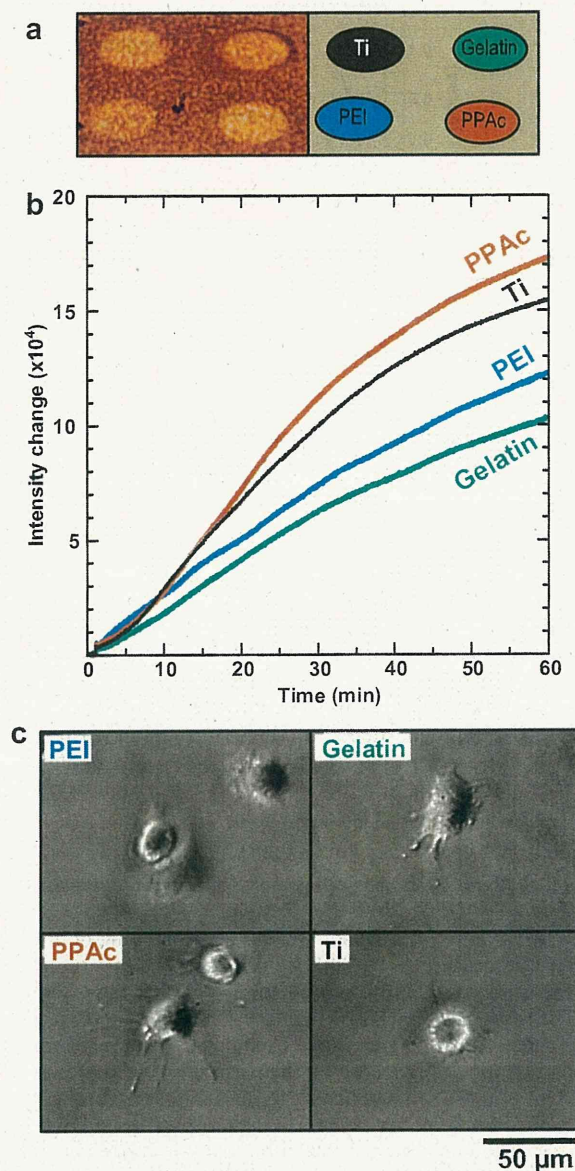
Fig. 9. MC3T3-E1 cell adhesion on the polymer-coated titanium array. (a) SPRI image of the array chip after 1 h incubation with cells. The four spots were titanium (passivation surface), PEI, gelatin, and PPAc, as shown in the schematic. (b) Real time assessment of MC3T3-E1 cell response on the polymer-coated titanium array by SPRI. (c) Phase contrast microscopy of MC3T3-E1 cell attachment.

Fig. 10. SPRI imaging of acid etching of the DDP treated titanium array chip. (a) The array chip of four 1 mm spots, of which two spots were titanium (passivation surface, black spots in the schematic), and the two other spots were treated with DDP (red spots in the schematic), amidst the ODTCS-treated titanium (blue surrounding area in the schematic). The SPRI image revealed that the DDP solution etched the ODTCS-treated titanium near the DDP spots. (b) The whole area, including the four spots and the surrounding area, were exposed to HCl/KCl buffer (pH 1.5), during which the SPR reflected light intensity was recorded in real time using SPRI.

and Ti spot clearly showed fewer filopodia without spread cell bodies. These results indicate that the cell response determined by SPRI did not correlate with the area over which the cells spread, but was at least in part due to some actions of the living cell. Although another measurement method to detect cell reactions is needed in combination, we propose that the study of early cell responses to titanium using SPRI could contribute to a better understanding of the early phases of osseointegration of titanium implants, leading to improved osseointegration therapy.

3.6. SPRI observation of the corrosion resistance of the titanium surface

The imaging potential of the Ti-SPR sensor was illustrated in a surface corrosion experiment involving exposure to a HCl/KCl buffered solutio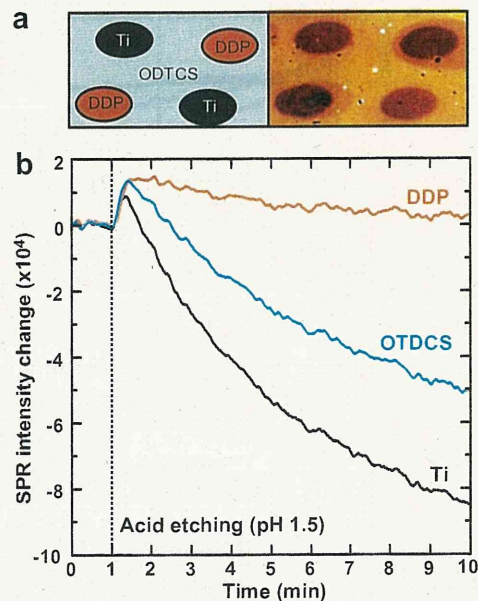n. DDP and ODTCS can be strongly immobilized on the surface as a self-assembled monolayer because they comprise long alkyl chains and surface-active head groups [40–41], and these immobilized layers are supposed to protect the titanium surface from acid. In Fig. 10a the SPRI image of a DDP-treated titanium array revealed that the DDP solution, which is acidic, etched the ODTCS-coated titanium around the DDP spots. The acid etching of titanium with HCl leads to the greatest corrosion at the titanium spot, slightly less of the OTDCS-coated surface, while the DDP spot appeared most resistant to HCl acid attack (Fig. 10b). This result suggests that these monolayers coated on a titanium surface are corrosion resistant, especially the DDP-treated surface.

4. Conclusions

The surfaces of titanium medical devices oxidize in air, the oxide forming a passivation layer. Our Ti-SPR sensor has a similar passivation layer to these devices because the titanium metal layer on the sensor oxides in a similar way. The Ti-SPR sensor could detect acid etching, biomolecule adsorption, cell reactions, and corrosion resistance of the titanium surface in real time.

The Ti-SPR sensor shows a broad applicability to study surface interactions with a titanium passivation layer. Within biomaterial sciences this instrument most obviously enables investigations of the surface chemistry and biomolecular aspects of the integration of titanium implants in human bone, especially to gain an insight into the earliest processes of protein adsorption and cell attachment, a scientifically important enigma that needs to be clarified in order to further ameliorate implant therapy in dental medicine and orthopedics. This sensor may also prove useful in studying the interactions of biomolecules and cells with other titanium-based medical devices used within the human body. Within materials sciences the process of corrosion could be studied in more depth to further improve the corrosion resistance of titanium-based

machines/equipment used in the marine and aerospace industries. Thus this innovative high resolution surface analytical tool could not only be employed to investigate the surface properties of titanium, but also to develop new materials with better surface treatment methods for titanium devices.

Acknowledgements

Appendix A. Figures with essential colour discrimination

Certain figures in this article, particularly Figure 1, is difficult to interpret in black and white. The full colour images can be found in the on-line version, at doi:10.1016/j.actbio.2011.11.025.

References

[1] Donachie MJ. Titanium: a technical guide. 2nd ed. Materials Park, OH: ASM International; 2000. p. 123–130.

[2] Ivasyshyn OM, Aleksandrov AV. Status of the titanium production, research, and applications in the CIS. Mater Sci 2008;44:311–27.

[3] Peacock DK. Effective design of high performance corrosion resistant systems for oceanic environments using titanium. Corros Rev 2000;18:295–330.

[4] Wake H, Takahashi H, Takimoto T, Takayanagi H, Ozawa K, Kadoi H, et al. Development of an electrochemical antifouling system for seawater cooling pipelines of power plants using titanium. Biotechnol Bioeng 2006;95:468–73.

[5] Maciver A, Hinge S, Andersen BJ, Nielsen JB. New trend in desalination for Japanese nuclear power plants, based on multiple effect distillation, with vertical titanium plate falling film heat transfer configuration. Desalination 2005;182:221–8.

[6] de Jonge LT, Leeuwenburgh SCG, Wolke JCG, Jansen JA. Organic–inorganic surface modifications for titanium implant surfaces. Pharm Res 2008;25:2357–69.

[7] Cilingiroglu M. Long-term effects of novel biolimus eluting DEVAX AXXESS Plus nitinol self-expanding stent in a porcine coronary model. Catheter Cardiovasc Interv 2006;68:271–9.

[8] Norlin A, Pan J, Leygraf C. Investigation of electrochemical behavior of stimulation/sensing materials for pacemaker electrode applications. I. Pt, Ti, and TiN coated electrodes. J Electrochem Soc 2005;152:J7–J15.

[9] Meirelles L, Albrektsson T, Kjellin P, Arvidsson A, Franke-Stenport V, Andersson M, et al. Bone reaction to nano hydroxyapatite modified titanium implants placed in a gap-healing model. J Biomed Mater Res Part B 2008;87A:624–31.

[10] Ku Y, Chung CP, Jang JH. The effect of the surface modification of titanium using a recombinant fragment of fibronectin and vitronectin on cell behavior. Biomaterials 2005;26:5153–7.

[11] Schuler M, Owen GR, Hamilton DW, de Wild M, Textor M, Brunette DM, et al. Biomimetic modification of titanium dental implant model surfaces using the RGDSP-peptide sequence: a cell morphology study. Biomaterials 2006;27:4003–15.

[12] Cochran DL, Schenk RK, Lussi A, Higginbottom FL, Buser D. Bone response to unloaded and loaded titanium implants with a sandblasted and acid-etched surface: a histometric study in the canine mandible. J Biomed Mater Res 1998;40:1–11.

[13] Langer R, Tirrell DA. Designing materials for biology and medicine. Nature 2004;428:487–92.

[14] Kretschmann E. Determination of the optical constants of metals by excitation of surface plasma. Z Phys 1971;241:313–24.

[15] Schasfoort RBM, Tudos A. Handbook of surface plasmon resonance. Cambridge: RSC Publishing; 2008. p. 15–34.

[16] Arima Y, Ishii R, Hirata I, Iwata H. Development of surface plasmon resonance imaging apparatus for high-throughput study of protein–surface interaction. e-J Surf Sci Nanotech 2006;4:201–7.

[17] Anker JN, Hall WP, Lyandres O, Shah NC, Zhao J, Van Duyne RP. Biosensing with plasmonic nanosensors. Nature Mater 2008;7:442–53.

[18] Liao HB, Xiao RF, Wang H, Wong KS, Wong GKL. Large third-order optical nonlinearity in Au:TiO2 composite films measured on a femtosecond time scale. Appl Phys Lett 1998;72:1817–9.

[19] Qi ZM, Honma I, Zhou H. Nanoporous leaky waveguide based chemical and biological sensors with broadband spectroscopy. Appl Phys Lett 2007;90:011102.

[20] Shinn M, Robertson WM. Surface plasmon-like sensor based on surface electromagnetic waves in a photonic band-gap material. Sens Actuators B Chem 2005;B105:360–4.

[21] Bernard A, Bosshard HR. Real-time monitoring of antigen–antibody recognition on a metal oxide surface by an optical grating coupler sensor. Eur J Biochem 1995;230:416–23.

[22] Plenet JC, Brioude A, Bernstein E, Lequevre F, Dumas J, Mugnier J. Densification of sol-gel TiO2 very thin films studied by SPR measurements. J Opt Mater 2000;13:411–5.

[23] Yao M, Tan CK, Tjin SC, Wolfe JC. Effects of intermediate dielectric films on multilayer surface plasmon resonance behavior. Acta Biomater 2008;4:2016–27.

[24] Hirata I, Morimoto Y, Murakami Y, Iwata H, Kitano E, Kitamura H, et al. Study of complement activation on well-defined surfaces using surface plasmon resonance. Colloid Surf B Biointerfaces 2000;18:285–92.

[25] Hirata I, Hioki Y, Toda M, Kitazawa T, Murakami Y, Kitano E, et al. Deposition of complement protein, C3b, on mixed self-assembled monolayers carrying surface hydroxyl and methyl groups studied by surface plasmon resonance. J Biomed Mater Res Part A 2003;66A:669–76.

[26] Knoll W. Polymer thin films and interfaces characterized with evanescent light. Makromol Chem 1991;192:2827–56.

[27] Azzam RMA, Bashara NM. Ellipsometry and polarized light. Amsterdam: North-Holland Personal Library; 1977. p. 283–363.

[28] Choi WS, Kim YM, Combs C, Frohman MA, Beaven MA. Phospholipases D1 and D2 regulate different phases of exocytosis in mast cells. J Immunol 2002;168:5682–9.

[29] Bower VE, Bates RG. The pH values of the Clark and Lubs buffer solutions at 25. J Res Nat Bureau Stand 1955;55:197–200.

[30] Dieblod U. The surface science of titanium dioxide. Surf Sci Rep 2003;48:53–229.

[31] Lu G, Bernasek SL, Schwartz J. Oxidation of a polycrystalline titanium surface by oxygen and water. Surf Sci 2000;458:80–90.

[32] Liu X, Chu PK, Ding C. Surface modification of titanium, titanium alloys, and related materials for biomedical applications. Mater Sci Eng R 2004;47:49–121.

[33] Safonova LP, Pryahin AA, Fadeeva JA, Shmukler LE. Viscosities, refractive indexes, and conductivities of phosphoric acid in N,N-dimethylformamide + water mixtures. J Chem Eng Data 2008;53:1381–6.

[34] Kokubo T, Kim HM, Kawashita M, Nakamura T. Bioactive metals: preparation and properties. J Mater Sci Mater Med 2004;15:99–107.

[35] Sul YT, Johansson CB, Kang Y, Jeon DG, Albrektsson T. Bone reactions to oxidized titanium implants with electrochemical anion sulphuric acid and phosphoric acid incorporation. Clin Implant Dent Relat Res 2002;4(2):78–87.

[36] Parfitt GD. The surface of titanium dioxide. Prog Surf Membr Sci 1976;11:181–226.

[37] Mani G, Johnson DM, Marton D, Feldman MD, Patel D, Ayon AA, et al. Drug delivery from gold and titanium surfaces using self-assembled monolayers. Biomaterials 2008;29:4561–73.

[38] Maekawa K, Yoshida Y, Mine A, Fujisawa T, Van Meerbeek B, Suzuki K, et al. Chemical interaction of polyphosphoric acid with titanium and its effect on human bone marrow derived mesenchymal stem cell behavior. J Biomed Mater Res 2007;82A:195–200.

[39] Yanase Y, Hiragun T, Kaneko S, Gould HJ, Greaves MW, Hide M. Detection of refractive index changes in individual living cells by means of surface plasmon resonance imaging. Biosens Bioelectron 2010;26:674–81.

[40] Spori DM, Venkataraman NV, Tosatti SGP, Durmaz F, Spencer ND, Zürcher S. Influence of alkyl chain length on phosphate self-assembled monolayers. Langmuir 2007;23(15):8053–60.

[41] Liang S, Chen M, Xue Q, Qi Y, Chen J. Site selective micro-patterned rutile TiO2 film through a seed layer deposition. J Colloid Interface Sci 2007;311(1):194–202.

Videoendoscopic assessment of swallowing function to predict the future incidence of pneumonia of the elderly

N. TAKAHASHI*[†], T. KIKUTANI*[‡], F. TAMURA*, M. GROHER[§] & T. KUBOKI[†]   *Rehabilitation Clinic for Speech and Swallowing Disorders, The Nippon Dental University School of Life Dentistry at Tokyo, Dental Hospital, Tokyo, [†]Department of Oral Rehabilitation and Regenerative Medicine, Okayama University Graduate School of Medicine, Dentistry and Pharmaceutical Sciences, Okayama, [‡]Division of Oral Rehabilitation, The Nippon Dental University Graduate School of Life Dentistry, Tokyo, Japan and [§]Department of Communicative Disorders, University of Redlands, Redlands, CA, USA

SUMMARY The purpose of the present study was to examine what dysphagic signs identified by video-endoscopy (VE) could predict the incidence of pneumonia and body weight loss in elderly patients living in nursing homes. This study was performed at six nursing care facilities in Japan from March 2007 to February 2009. The 148 subjects (85·1 ± 8·0 years, male/female: 43/105) were evaluated for their feeding and swallowing movements by clinical and VE examinations during the consumption of a regular meal. The VE examination items included the existence/absence of pharyngeal residue, laryngeal penetration, and aspiration of food and saliva. The patients were followed-up for 3 months with individualized feeding therapy based on the results of the clinical/VE examination at baseline, and the incidence of pneumonia was examined as the primary outcome. In patients without pneumonia, the body weight change was also measured as a secondary outcome. The risk factors for pneumonia and body weight loss (of 3% or more) were identified among the clinical/VE examination items by a Cox proportional hazard analysis. Even with elaborative feeding therapy, 12 (8·1%) of the 148 patients developed pneumonia during the 3 months follow-up period. The existence of signs of 'silent aspiration of saliva' or 'aspiration of saliva' detected by VE examination was a significant risk factor for both pneumonia and a body weight loss of 3% or more. This study shows that 'aspiration of saliva' detected by VE is a significant risk factor for both pneumonia and body weight loss in elderly patients living in nursing homes.

KEYWORDS: videoendoscopy, aspiration-related pneumonia, dysphagia, aspiration of saliva, body weight loss

Accepted for publication 14 December 2011

Introduction

Dependent elderly patients are at high risk for feeding and swallowing disorders as a consequence of disease and/or aging (1–3). Studies done in long-term care facilities have shown a prevalence of such disorders ranging from 60% to 87% (4, 5). Among the various disorders, special attention has been given to dysphagia because it may lead to malnutrition with immune system compromise, dehydration, asphyxiation, or even aspiration pneumonia (1–3). Moreover, a previous follow-up study of patients with dysphagia in such care facilities revealed an incidence of pneumonia of 43% and a mortality rate of 45% at 1 year following the detection of their swallowing disorder (6). Therefore, clinicians should be able to identify dysphagia in order to predict those patients at risk of developing complications secondary to dysphagia, as well as to develop and implement a rehabilitation plan stressing prevention and compensation.

Videofluorography (VF) has been regarded as the most popular adjunctive instrument for the

examination of patients with suspected oropharyngeal dysphagia. Previous studies have examined the use of VF as a means to predict those at risk for dysphagia and its complications (7, 8). For instance, Mann *et al.* (7) found that the single best independent predictor for chest infection following an acute stroke was a delayed or absent swallowing response in acute stroke patients. Teraoka *et al.* (8) found that the single best predictor of oral intake in post-stroke patients with dysphagia was the presence of aspiration detected by VF assessment. Nevertheless, one major disadvantage of VF for patients living in long-term care facilities is that the patients need to be transported to a hospital setting, which is sometimes inconvenient or may disorientate the patient because of the sudden change in the environment. Other disadvantages are related to the exposure to x-ray radiation and the risk of aspiration during VF assessment in some patients with severe physical or mental alterations (9).

On the other hand, videoendoscopic (VE) examination of swallowing allows for easy assessment of patients in their usual environment because the instrument is portable and does not require a radiology suite (10). Additionally, although VE is most useful for the examination of the integrity of the upper airway before and after a swallow response, it enables the evaluation of the tongue function during mastication and deglutition, as well as the detection of aspiration by the objective visualization of the airway (11, 12).

Videoendoscopic examination has been shown to successfully estimate the existence of accumulated oropharyngeal secretions, thus resulting in excellent prediction of aspiration (13, 14). In addition, Ota *et al.* (15) reported that the secretion scale based on the VE examination is a useful evaluation tool for predicting not only aspiration, but also pneumonia, in acute-phase dysphagic stroke patients. Furthermore, Link *et al.* (16) reported that there was a relationship between the VE-based pooled hypopharyngeal secretions, laryngeal penetration, aspiration and recurrent pneumonia with neurological disorders in pediatric patients. It is therefore evident that VE is the best tool to examine pooled hypopharyngeal secretions, laryngeal penetration, and aspiration. Therefore, even though the agreement rate between the VF and VE findings on dysphagia was shown to be high (90%) (17), VE examinations are becoming increasingly popular for examining the aspiration of saliva and food at the bedside and in long-term care facilities (17, 18).

In a prospective study with acute stroke patients, Lim *et al.* (19) found a strong association between aspiration detected by VE and the development of aspiration pneumonia. However, the predictors of aspiration pneumonia in dependent elderly patients with dysphagia in long-term care facilities have not been sufficiently investigated using VE. Therefore, the purpose of this prospective cohort study was to investigate whether the dysphagic signs identified by VE were risk factors for pneumonia and body weight loss in patients living in long-term care facilities.

Materials and methods

Subjects

Six hundred and forty-seven inpatients were initially identified from six nursing care facilities in Tokyo, Japan from March 2007 to February 2009 (Fig. 1). All patients, except for 28 subjects who were tube-fed, were screened for dysphagia by a check-list given to the patient's caregiver. The screening check-list contained 11 items: pooling of food, uncomfortable feeling in the throat, previous history of asphyxiation, previous history of aspiration, previous history of pneumonia, increased phlegm production, choking on saliva, choking on food, choking after a meal, prolongation of their eating time, and insufficient intake. The 171 patients who had at least one item checked positively by the caregiver were suspected to have dysphagia and comprised the intended sample population. However, 23 patients were excluded because of cognitive failure or refusal to participate in this study. Consequently, the final study population consisted of 148 patients (male/female: 43/105) with a mean age of 85·1 ± 8·0 years and an age range from 59 to 100 years. The protocol for this study was approved by the Ethics Committee of the Nippon Dental University School of Life Dentistry at Tokyo (#08-10).

Baseline measurements and feeding therapy

At the baseline measurement, a medical doctor assessed the patients' general health condition, and none of the patients fulfilled the Mann's criteria (7) for a diagnosis of pneumonia, that is, the presence of at least three of the following signs and symptoms: fever >38 °C, productive cough with sputum, tachypnea higher than 22 breaths per minute, inspiratory crackles,
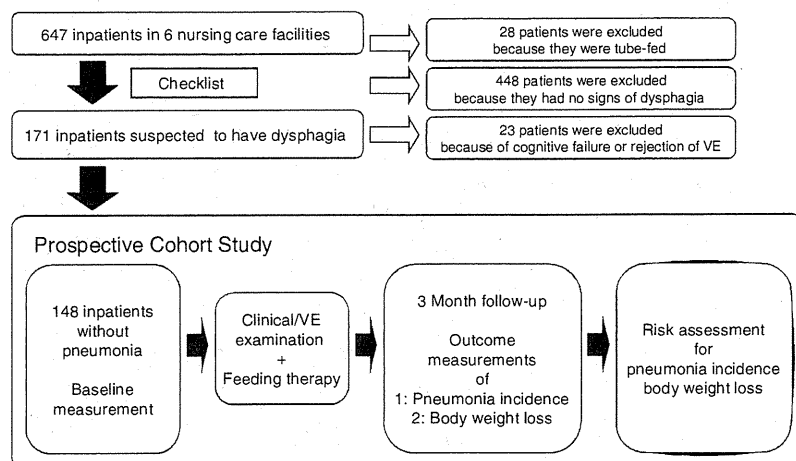
Fig. 1. The sampling process used for this study.

an abnormal chest x-ray, or positive gram staining and cultures.

All included subjects had their eating ability and dysphagic signs and symptoms evaluated clinically according to a clinical examination form regarding the signs and symptoms of dysphagia (spilling food, pooling food, oral food residue after a swallow, inability to open the mouth, choking/coughing, increased phlegm while eating, dyspnea, wet hoarseness, other), the hand and mouth coordination during the meal (feeding posture, prolongation of eating time) and the caregiver's technique used for feeding assistance.

In addition, each patient's swallowing function was examined by VE, which consisted of a flexible endoscope (ENF-V2*) connected to a high-intensity compact light source (CLH-SC*) and a video recorder (OTV-SC*).The endoscope was passed transnasally to the hypopharynx at a vantage point that provided a full view of the laryngeal vestibule, and was kept in place for a period of 10–15 min to assess the patient's eating ability, or saliva swallows when the patient was not consuming a meal. The patients were examined in their usual eating position, that is, the ambulatory patients were seating in the upright position, while the bed-bound patients were sitting on a bed. All swallows were recorded on videotapes for the further analyses by experienced physicians familiar with endoscopic swallowing studies and who were blinded to the intentions of the study. Each patient's video-recording data were reviewed for the

*Olympus Corporation, Tokyo, Japan.

presence or absence of pharyngeal residue, and penetration and aspiration of food or saliva. 'Penetration' was defined as a passage of material into the larynx that does not pass below the vocal folds, while 'aspiration' was defined as passage of material below the level of the vocal folds. In cases where the aspiration of food or saliva did not induce a cough, it was defined as 'silent aspiration' according to the criteria proposed by Rosenbek et al. (1996) (20). To assess the inter-rater reliability of the swallowing evaluations, the three investigators who were unaware of the original evaluation results, separately reviewed a random 10% sample of these evaluations. The overall agreement rate between investigators was substantial according to the Landis and Koch criteria (21) (kappa coefficient = 0·660).

On the basis of these aforementioned evaluations, the patients received various feeding therapies (22) during the follow-up period, for example, confirmation of feeding conditions [76 patients (51·4%) of 148 patients, multiple answers possible], appropriate feeding assistance [69 patients (46·6%)], food modification [32 patients (21·6%)], modification in feeding posture [19 patients (12·8%)] and modification in food intake [four patients (2·0%)] for 3 months. Food modification involved changing the dietary consistency. We modified the food and liquid texture individually according to the National Dysphagia Diet recommendations (23). Food intake and feeding assistance required modifications to accommodate the individual needs of the patients, such as changes in the rate and amount of the food consumed, appropriate utensils and the

method used for self-feeding (22). Modifications in the feeding posture were applied in order to maximize the physical capabilities and improve swallowing, and involved strategies such as head-turn or chin-tuck maneuvers or whole body-positioning strategies including the patient tilting to the side or back, side-lying, or maintaining an upright posture (22). All patients received oral health care after every meal by the caregiver who was instructed once a week about the oral care procedures by a dental hygienist. Caregivers cleaned each patient's oral cavity using a toothbrush for approximately 5 min after each meal. The brushing was carried out as usual for daily tooth brushing without paste, and included brushing the palatal and mandibular mucosa and tongue dorsum. Dentures were also cleaned with a denture brush every day.

The 3 month follow-up and outcome measurement

The first outcome variable after 3 months of follow-up was the incidence of pneumonia diagnosed according to the same criteria applied at the baseline measurement. Once the patients received a diagnosis of pneumonia, they were sent to a local hospital for treatment, without exception. Consequently, their oral feeding was prohibited to prevent further aspiration pneumonia and their body weight typically decreased as a result (24). The incidence of pneumonia and body weight loss were therefore strongly correlated after the development of pneumonia. Thus, when pneumonia was identified, follow-up measurements of the patient's body weight were terminated.

The second outcome variable during the follow-up period was a change in body weight demonstrated by monthly measurements. Since there is a close relationship between pneumonia and body weight loss, the incidence of body weight loss of 3% or more was examined in patients who had not been diagnosed with pneumonia during the 3 months of follow-up. Once the patients developed a body weight loss of 3% or more, the patients received some form of nutrition therapy, and thus, the follow-up observation was terminated.

Statistical analysis

A survival curve of the patients who had not been diagnosed with pneumonia was drawn for a Kaplan–Meier analysis. According to the presence/absence of

pneumonia during the 3 months of follow-up, we divided the final sample population into pneumonia and non-pneumonia sub-groups, and performed a t-test, chi-square analysis or Fisher's exact test to analyse the differences between the two groups.

Similarly, a survival curve of those patients who had not lost more than 3% of their body weight was drawn for a Kaplan–Meier analysis (outcome event: the incidence of body weight loss of 3% or more). Differences between the weight gain/no change sub-group (body weight gain, or a small weight loss of no more than 3% of the initial body weight) and the weight loss group (body weight loss of 3% or more (10, 25)) were analysed with the same statistical tests utilized for the incidence of pneumonia.

Additionally, a Cox proportional hazard analysis was performed to identify the risk factors for the incidence of pneumonia and the body weight loss of 3% or more. The analysed predictors were age, self-feeding ability, the Barthel activities of daily living (ADL) index, a body mass index (BMI) lower than 18·5, pharyngeal residue, laryngeal penetration, aspiration of food and aspiration of saliva. Regarding the aspiration of food or saliva, the data were handled as ordinal variables (negative, positive, positive as silent aspiration). The data were analyzed with the Statistical Package for the Social Sciences software program (SPSS version 15.0[†]). A P-value $<0·05$ was considered to be statistically significant.

Results

Baseline condition of the patients

Examination of the medical conditions of the initial 148 patients showed the presence of a prior stroke in 83 (comorbidity admitted) (56·1%), dementia in 74 (50·0%), Parkinson's disease in 10 (6·8%), cardiovascular disease in 10 (6·8%), hypertension in 8 (5·4%), previous pneumonia in 5 (3·4%), diabetes mellitus in 3 (2·0%), fractures in 3 (2·0%) and other comorbidities in 14 patients (9·5%).

The clinical examination regarding the eating ability and signs and symptoms of dysphagia before the VE evaluation showed choking/coughing in 110 out of 148 patients (multiple choice admitted), pooling of food in 28, prolongation of the eating time in nine, inability to

open the mouth in two, and spilling of food in one patient.

The VE evaluation detected pharyngeal residue in 97 (65·5%) out of the 148 patients, laryngeal penetration in 67 (45·3%), aspiration of food in 41 (27·7%), silent aspiration of food in 19 (12·8%), aspiration of saliva in 8 (5·41%), and silent aspiration of saliva in 10 (6·76%) patients (Table 1).

Risk factors for pneumonia and body weight loss

Even with elaborative feeding therapy, during the 3 months of follow-up after the baseline measurement, 12 (8·1%) of the 148 patients developed pneumonia (Fig. 2). In addition, among the non-pneumonia patients, 90 (66·2%) of them presented with weight gain, no change or weight loss of 3% or less (weight gain/no change group), while 46 patients (33·8%) lost 3% or more of their body weight (weight loss group) (Fig. 3).

The differences between the pneumonia and non-pneumonia groups concerning the clinical/demographic data and the dysphagic signs detected by VE are shown in Table 1. The unpaired t-test showed that there were no significant differences in the patient age ($P = 0·505$), gender ($P = 0·244$), self-feeding ability ($P = 0·419$), number of patients with a BMI lower than 18·5 ($P = 0·190$), and the Barthel Index ($P = 0·060$)

between the subjects with and without pneumonia. On the other hand, there was a significant difference in the frequency of 'aspiration of saliva' between the pneumonia and non-pneumonia patients ($P = 0·026$). In contrast, a comparison between the body weight gain/no change and body weight loss groups showed that there were no significant differences concerning any of the analysed variables (Table 2).

The results of the Cox proportional hazard analysis revealed that a sign of the 'aspiration of saliva' detected by VE was a significant risk factor for pneumonia (Table 3) and for a body weight loss of 3% or more (Table 4).

Discussions

The presence of aspiration-related pneumonia is known to be associated with a high mortality rate in the elderly. Patients in nursing homes may have a higher incidence of pneumonia because of their multiple underlying diseases, which may lead to immunosuppression, excessive use of medications, generalized decreased functional status, as well as factors related to malfunctioning of the masticatory and oroprharyngeal systems and inadequate oral care. In particular, dysphagia is known to be strongly associated with aspiration pneumonia. Teramoto *et al.* (26). reported

Table 1. The relationship between the clinical/VE signs and the incidence of pneumonia

	Total subjects	No pneumonia ($n = 136$)	Pneumonia ($n = 12$)	P-value
Age (mean ± s.d.)	148	85·0 ± 8·1	86·8 ± 5·4	0·505[†]
Male/female	148	38/98	5/7	0·244[††]
Self-feeding (yes/no)	148	47/89	5/7	0·419[††]
Barthel Index (mean ± s.d.)	116*	13·1 ± 18·1	7·2 ± 7·12	0·060[†]
BMI < 18·5**	118**	43/110 (39·1%)	5/8 (62·5%)	0·190[††]
Pharyngeal residue	148	88 (64·7%)	9 (75·0%)	0·354[††]
Laryngeal penetration	148	62 (45·6%)	5 (41·7%)	0·519[††]
Aspiration of food	148			0·326[††]
Silent aspiration	19	19	0	
Aspiration	41	38	3	
NA	88	79	9	
Aspiration of saliva	148			0·026[††]
Silent aspiration	10	7	3	
Aspiration	8	7	1	
NA	130	122	8	

*Of 116 patients, 107 were in the no pneumonia group and nine were in the pneumonia group.
**Of 118 patients, 110 were in the no pneumonia group and eight were in the pneumonia group.
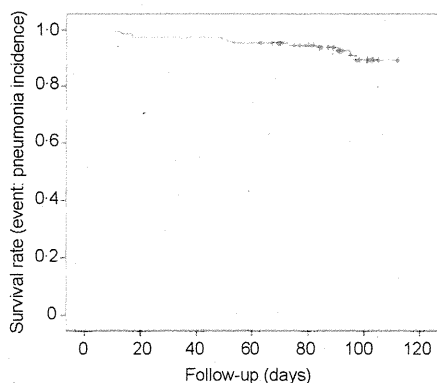[†]T-test.
[††]Chi-square test.

Fig. 2. The survival curve of the patients who did not suffer from pneumonia. The survival curve was drawn for a Kaplan–Meier analysis (outcome event: incidence of pneumonia).
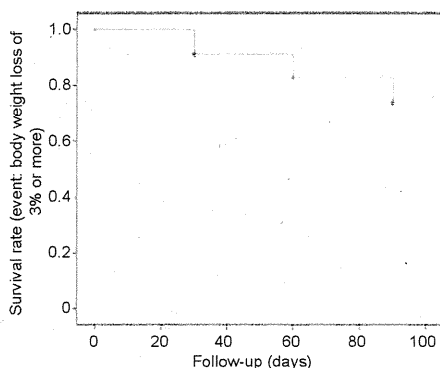

Fig. 3. The survival curve of the patients who did not suffer from a body weight loss of 3% or more. The survival curve was drawn for a Kaplan–Meier analysis (outcome event: incidence of body weight loss of 3% or more).

that 70% of the pneumonia in the elderly occurred due to aspiration, and Yamaya *et al.* (27). reported a high prevalence of silent aspiration in older persons leading to the deterioration of swallowing function due to cerebrovascular disease. In a previous study, Doggett *et al.* (28) estimated that approximately 43–54% of stroke patients have dysphagia and aspiration of food or saliva, and that approximately 37% of these patients would develop aspiration-related pneumonia.

In this present study, penetration and aspiration (apparent or silent) was observed in 67 subjects (45·2%) and 60 subjects (40·5%), respectively. The prevalence of aspiration found in this investigation was relatively high compared to previous studies utilizing VE examination (29%) (29), but was similar to the range observed in a previous review article where it was

reported to occur in 15–39% of subacute dysphagic stroke patients (30). According to this review, the exact prevalence of aspiration remains unknown because of the differences in the size and methodology used in the existing studies.

The incidence of pneumonia was 12 (8·1%) among the 148 subjects (Table 1), which is in accordance with the study by Lim *et al.* (19), who reported that five patients (10%) developed pneumonia during their inpatient stay, and that all of them were at risk of aspiration of saliva or food as determined by a VE examination. On the other hand, Croghan *et al.* (6) reported that 55% of their nursing home patients presented with aspiration on VF examination, and 43% developed pneumonia.

One possible reason for such a discrepancy in the association of pneumonia and aspiration or penetration could be due to the technique (VE vs. VF) utilized to assess the swallowing disorders. Although a number of methods have been used to detect the symptoms of dysphagia, it is very difficult to evaluate 'silent aspiration of saliva' with a bedside clinical assessment alone, because it has been shown that it is missed in up to 40% of the patients aspirating silently (31, 32). At present, VF and VE are regarded as the best methods to evaluate swallowing function. In particular, VF has been used as a gold standard to evaluate swallowing because it can detect aspiration. However, it may not be as accurate in identifying 'silent aspiration of saliva', as compared to VE, because the latter enables direct visualization of the aspiration of saliva (18, 33, 34). Kelly *et al.* (35) reported that penetration and aspiration are perceived more sensitively in VE images than in VF images of the same swallows. It is also well known that VE can identify the microaspiration and aspiration of secretions with a high reliability, whereas VF cannot (36, 37). Additional advantages of VE are related to its application. Inpatients may become agitated or fatigued in the radiology suite or may not respond well to the taste of barium-coated boluses, or may even reject the radiation exposure, limiting the applications of VF. Videoendoscopy allows the patient's examination to be performed regardless of his/her altered mental status or immobility (38). Finally, Wu *et al.* (39) stated that VE is conclusively a safe, more efficient and sensitive method than VF for evaluating swallowing.

Another reason for the discrepancy could be the effect of the feeding therapy provided in this study, which could have reduced the symptoms of dysphagia,

Table 2. The relationship between the clinical/VE signs and the change in body weight

	Total subjects	Gain/no change (n = 90)	Weight loss (n = 46)	P-value
Age (mean ± s.d.)	136	84·6 ± 8·0	85·7 ± 8·6	0·464[†]
Male/female	136	25/65	13/33	0·553[††]
Self-feeding (yes/no)	136	29/61	16/30	0·454[††]
Barthel Index (mean ± s.d.)	107*	14·9 ± 18·7	9·6 ± 17·0	0·163[†]
BMI < 18·5	110**	30/74 (40·5%)	13/36 (36·1%)	0·655[††]
Pharyngeal residue	136	61 (67·8%)	27 (58·7%)	0·294[††]
Laryngeal penetration	136	44 (48·9%)	18 (39·1%)	0·2797[††]
Aspiration of food	136			0·975[††]
Silent aspiration	19	13	6	
Aspiration	38	25	13	
No aspiration	79	52	27	
Aspiration of saliva	136			0·342[††]
Silent aspiration	7	4	3	
Aspiration	7	3	4	
No aspiration	122	83	39	

Weight loss was diagnosed as the loss of 3% or more of the body weight from the baseline measurement.
*Of the 107 patients, 72 were in the gain/no change group and 35 were in the weight loss group.
**Of the 110 patients, 74 were in the gain/no change group and 36 were in the weight loss group.
[†]T-test.
[††]Chi-square test.

Table 3. The results of the Cox proportional hazard analysis for the possible predictors of the incidence of pneumonia

Predictors	B	P-value	HR	95% CI
Age	0·011	0·860	1·011	0·900–1·135
Self-feeding	0·105	0·909	1·111	0·182–6·785
Barthel Index	−0·010	0·769	0·990	0·927–1·057
BMI < 18·5	2·064	0·070	7·874	0·844–73·440
Pharyngeal residue	−0·621	0·615	0·537	0·048–6·067
Laryngeal penetration	0·571	0·642	1·771	0·160–19·644
Aspiration of food (negative/positive/ positive with SA)	−0·216	0·830	0·805	0·112–5·794
Aspiration of saliva (negative/positive/ positive with SA)	1·290	0·025	3·634	1·174–11·242

HR, hazard ratio; CI, confidence interval; SA, silent aspiration.

Table 4. The results of the Cox proportional hazard analysis for the possible predictors of a body weight loss of 3% or more

Predictors	B	P-value	HR	95% CI
Age	0·019	0·448	1·019	0·971–1·070
Self-feeding	0·530	0·228	1·698	0·718–4·014
Barthel Index	0·000	0·992	1·000	0·976–1·025
BMI < 18·5	0·859	0·032	2·362	1·074–5·191
Pharyngeal residue	−0·060	0·896	0·942	0·381–2·325
Laryngeal penetration	0·019	0·970	1·019	0·374–2·780
Aspiration of food (negative/positive/ positive with SA)	−0·203	0·569	0·816	0·405–1·644
Aspiration of saliva (negative/positive/ positive with SA)	1·186	0·000	3·275	1·828–5·866

HR, hazard ratio; CI, confidence interval; SA, silent aspiration.

pharyngeal residue, laryngeal penetration, and aspiration of food, as demonstrated by the fact that 66% of the subjects were able to increase their body weight or keep the body weight loss to within 3%. Nevertheless, a detailed analysis of the effectiveness of feeding therapy on the reduction of the symptoms of dysphagia could not be performed, because it was beyond the scope of this study.

Additionally, the differences in the target populations and their respective medical conditions could also have affected the overall incidence of pneumonia. This study gathered a heterogeneous patient population consisting of patients presenting with well-known disorders/diseases associated with the symptoms of dysphagia (e.g. stroke, Parkinson's disease, dementia) as well as other non-debilitating diseases/disorders (hypertension, fractures). On the other hand, a strong point in this study was the inclusion of a relatively high number of subjects from six nursing care facilities, which was large compared to other follow-up studies. Therefore,